Parallel Signaling Pathways in Endothelin-1–Induced Proliferation of U373MG Astrocytoma Cells

SHAOQING HE, ADNAN DIBAS, THOMAS YORIO,[1] AND GANESH PRASANNA[2]

Department of Pharmacology and Neuroscience, University of North Texas Health Science Center at Fort Worth, Fort Worth, Texas 76107

Endothelin-1 (ET-1) is a potent mitogen for many cells, especially when its levels are elevated under pathological conditions, as seen in tumor cell progression and astroglial activation in neuropathies. While ET-1 is known to cause astroglial proliferation, in the present study, multiple signaling pathways involved in ET-1–mediated astrocyte proliferation were characterized. Treatment with PD98059 and U0126 (MEK inhibitors) inhibited not only ET-1–induced cell proliferation but also ET-1–activated phosphorylation of extracellular signal–regulated protein kinase 1/2 (ERK1/2) in U373MG astrocytoma cells. Whereas the nonselective protein kinase C (PKC) inhibitor chelerythrine attenuated ET-1–induced cell proliferation, it was unable to block ET-1–induced ERK phosphorylation. However, ET-1 did not activate conventional or novel PKCs and did not elevate intracellular calcium. In addition, U73122 (a selective phospholipase C inhibitor), FTI-277 (an H-Ras inhibitor), as well as protein tyrosine kinase inhibitors also did not abolish ET-1–induced ERK1/2 phosphorylation. ET-1 treatment increased the activity of total Ras but not H-Ras. The phosphoinositide 3-kinase (PI3K) pathway appeared to be involved in signal transduction induced by ET-1, but it did not appear to participate in cross talk with the mitogen-activated protein kinase (MAPK) pathway. Activated ET receptors did not propagate signals either through protein tyrosine kinases or transactivation of EGF receptor tyrosine kinases, which typically trigger Ras-Raf-MAPK pathways. The results indicate that ET-1 stimulates cell proliferation by the activation of MAPK-, PKC-, and PI3K-dependent pathways that appear to function in a parallel manner. There is no apparent, direct "cross talk" between these pathways in U373MG cells, but rather, they might act on the independent but necessary components of the mitogenic effects of ET-1. Exp Biol Med 232:370–384, 2007

Key words: astrocyte; endothelin-1; cell proliferation; signal transduction

Introduction

Astrocyte activation and proliferation has been demonstrated in several neuropathies, including ocular neuropathy and brain astrocyte tumor progression(1–6). Astrogliosis is defined as an abnormal increase in the number of astrocytes due to the destruction of nearby neurons and is characterized by exhibiting proliferative and hypertrophic responses (7, 8). Typically, astrogliosis is seen following neurotrauma, hypoxia/ischemia, and other pathologies and is manifested by a dramatic change in the expression of extracellular matrix profile, which in most cases results in a glial scar (9).

Endothelins, a family of vasoactive peptides that include endothelin-1 (ET-1), are implicated in numerous physiological and pathological conditions, including hypertension, cardiac failure, brain and myocardial infarctions, disseminated intravascular coagulation, Alzheimer's disease, and glaucoma (1, 10, 11). ET-1, the predominant isoform of ET, is a potent mitogen in many cells, including smooth muscle cells, fibroblasts, and astrocytes (7, 12–16). ET receptors, ET_A and ET_B, are also expressed in many types of cells in the central nervous system (CNS), with ET_B as the predominant receptor in the CNS (17). The changes in ET-1 expression and/or regulation of ET receptors appear to play an important role in CNS astrogliosis (18, 19).

The mitogen-activated protein kinase (MAPK) signaling pathway is an important pathway in governing cell proliferation, differentiation, and cell death (20, 21). In response to diverse stimuli, such as growth factors, stresses, etc., components of the MAPK become phosphorylated and activated, consequently triggering signaling cascades, ultimately resulting in gene transcription (21, 22). The p44 and

This work was supported by the National Institutes of Health grant EY11979 (T.Y.); a Texas Higher Education Coordination Board Advanced Technology grant (T.Y.); a University of North Texas Health Science Center Intramural grant (G.P.); and American Health Assistance Foundation grant G200006P (G.P.).

[1] To whom correspondence should be addressed at Department of Pharmacology and Neuroscience, University of North Texas Health Science Center at Fort Worth, Fort Worth, TX 76107. E-mail: yoriot@hsc.unt.edu

[2] Current address: Research Pharmacology, Pfizer Global R&D, La Jolla, CA.

Received May 17, 2006.
Accepted September 8, 2006.

1535-3702/07/2323-0370$15.00

p42 MAPK/extracellular signal–regulated protein kinase 1/2 (ERK1/2) is an important member of the MAPK family that is involved in cell growth, proliferation, and differentiation (21–23).

ET-1, through its ET_A and ET_B receptors, activates the MAPK pathway by phosphorylation of ERK1/2 in many types of cells, including smooth muscle cells, fibroblasts, and astrocytes (1, 19, 21, 24). These studies indicated that ET_A receptor–mediated mitogenic activity occurred predominantly through two pathways: protein kinase C (PKC)– and phosphoinositide 3-kinase (PI3K)–dependent pathways, both of which stimulate MAPK (25–27), whereas activation of ET_B receptor–mediated mitogenic activity appears to utilize PKC-independent pathways (21–24). PKC can also act upstream of the MAPK pathway *via* activation of Ras and Raf to influence cell proliferation through the classical Ras-Raf-MEK-ERK pathways identified through activation of growth factor receptors (23, 28, 29).

Previously, we have shown that ET-1 induces cell proliferation in human U373MG astrocytoma cells and in human optic nerve head astrocytes in culture (7). However, little is known about the ET-1–induced signaling pathways responsible for astrocyte cell proliferation, specifically in U373MG astrocytoma cells, which are extremely invasive tumorigenic cells in the CNS. Presently the mechanism by which ET-1 stimulates the proliferation of human U373MG astrocytoma cells is addressed, and the hypothesis that MAPK and PKC pathways are both involved was tested. Our study indicated that PKC, MAPK, and PI3K pathways are directly involved in astrocyte cell proliferation induced by ET-1 and that the activation of ERK1/2 does not appear to involve a cross talk between c/nPKC (conventional and novel PKC) and PI3K pathways.

Materials and Methods

Materials. Dulbecco's modified Eagle's medium (DMEM; catalog no. 11995–040) and penicillin-streptomycin-glutamine were obtained from Gibco (Rockville, MD). Fetal bovine serum (FBS) was obtained from Hyclone Laboratories, Inc. (Logan, UT). PD98059, U0126, chelerythrine, RO-31–8425, genistein, AG82, herbimycin, LY294002, and FTI-277 were purchased from Calbiochem (La Jolla, CA). Rabbit anti-ERK1/2 polyclonal antibody, rabbit anti-phospho-ERK1/2 (Thr202/Tyr 204) polyclonal antibody, rabbit anti-phospho-pan-PKC polyclonal antibody, and rabbit anti-phospho-Akt (Ser 473) polyclonal antibody were purchased from Cell Signaling Technology (Beverly, MA); H-Ras plasmid cDNA and H-RasS17N dominant negative cDNA were obtained from Guthrie cDNA Resource Center (Sayre, PA); EZ-Detect-Ras activity kits were from Pierce Biotechnology, Inc. (Rockford, IL); Fura-2/AM was purchased from Molecular Probes, Inc. (Eugene, OR); and phorbol 12-myristate 13-acetate (PMA), phorbol 12-monomyristate (PMM), and all other chemicals were purchased from Sigma Chemical Co. (St. Louis, MO). ET-1, BQ610, and BQ788 were obtained from Peninsula Laboratories (Belmont, CA).

Cell Cultures. U373MG cells (human astrocytoma glioblastoma) obtained from the American Type Culture Collection (ATCC; Manassas, VA) were maintained in DMEM containing 10% FBS supplemented with 10 U/ml penicillin, 100 μg/ml streptomycin, and 0.3 μg/ml glutamine under humidified 5% CO_2 at 37°C. For plasmid cDNA transfection, cells were cultured to 80% confluence, and the media were changed to serum-free DMEM without penicillin and streptomycin. For the experiment with DNA transfection, in each 100-mm–dish cell culture, 10 μg of plasmid cDNA was used for transfection with lipofectamine 2000 (Invitrogen, Inc., Carlsbad, CA), according to the instructions of the manufacturer. After 8 hrs, cells were washed with serum-free DMEM and cultured for 24 hrs before treatment.

Western Blot. U373MG cells were cultured in 100-mm dishes to confluence; 24 hrs later the media were changed to serum-free DMEM, cells were pretreated with different inhibitors/ET receptor antagonists for 30 mins, and then cells were stimulated with 100 n*M* ET-1 for the various time periods described herein. The reaction was stopped by adding ice-cold phosphate-buffered saline (PBS). The cells were scraped and lysed in a lysis buffer (50 m*M* Tris, pH 8.0; 100 m*M* NaCl; 1 m*M* EGTA; 1 m*M* sodium orthovanadate; 5 μ*M* $ZnCl_2$; 50 m*M* NaF; 1 m*M* phenylmethylsulfonyl fluoride; 10 μg/ml aprotinin, leupeptin, and soybean trypsin inhibitor; 1% (v/v) NP-40; and 1% (v/v) triton X-100). Total cell lysate was applied to 10% sodium dodecyl sulfate–polyacrylamide gel electrophoresis (SDS-PAGE) and transferred to nitrocellulose membranes (Protran Bioscience, Keene, NH). The transferred membranes were blocked with 5% nonfat milk in Tris-buffered saline/Tween (10 m*M* Tris-HCl, pH 8.0; 150 m*M* NaCl; and 0.5% Tween 20) for 1 hr and incubated with primary antibody for 1 hr at room temperature or overnight at 4°C. Horseradish peroxidase–conjugated anti-mouse or anti-rabbit IgG antibodies (Amersham Pharmacia Biotech, Piscataway, NJ) was used as a secondary antibody, and the enhanced chemiluminescence reagents (Amersham Pharmacia Biotech) were used for the blotting detection. X-ray films (Kodak, Rochester, NY) were exposed and scanned using a Hewlett-Packard scanner. Density of bands was determined by the software Scion Image (Scion Corporation, Frederick, Maryland). The error bars shown in the figures represent the standard deviation of the mean from the triplicate of a representative experiment.

Cell Proliferation Assays. Formazan-MTT and [methyl-^{3}H]thymidine incorporation assays were used in the present study. Formazan-MTT assay (Promega, Madison, WI) was performed as previously described (2, 7). U373MG cells were seeded in 96-well plates in DMEM containing 10% FBS at a concentration of 1000 cells per well. On the second day, the media was changed to serum-free DMEM, U373MG cells were pretreated with drugs for 30 mins and then stimulated with or without 100 n*M* ET-1

for 24 hrs. The media was aspirated, and 120 μl of a formazan mixed reagent (100 μl pre-warmed SF-DMEM and 20 μl formazan one solution reagent) was added per well. Cells were incubated at 37°C in 5% CO_2, and we detected O.D. value at 490-nm wavelength using the plate reader (SpectraMax 340pc, Molecular Devices, Sunnyvale, CA).

A [^{3}H]thymidine incorporation assay was also performed, as previously described (30). Briefly, cells were seeded at 1×10^5 cells per well in 24-well plates in quadruplicate wells. After 8 hrs the cells were placed in serum-free medium for 24 hrs. ET-1 was then added at a final concentration of 100 n*M* for 16 hrs; this step was followed by addition of [^{3}H]thymidine (1 μCi/well; Amersham Pharmacia Biotech) for 8 hrs. Cells were incubated with ice-cold 5% trichloroacetic acid for 30 mins and were later washed with ice-cold PBS. Cells were then washed once with PBS followed by incubation with 0.5 ml of lysis solution (0.5 *M* NaOH/0.5% SDS). Lysis solution was transferred into a scintillation vial containing scintillation cocktail and vials were counted in a beta counter. For inhibitor studies, cells were pretreated for 30 mins followed by addition of ET-1 and [^{3}H]thymidine, as described above.

PKC Translocation Assay. To determine the translocation of PKC isoforms as a mean to demonstrate PKC activation, the membrane and the cytosol fractions were isolated from cell lysates using previously described procedures (31). U373MG astrocytoma cells treated with different drugs were harvested and sonicated 15 times with 1-sec sonication and 1-sec intervals in ice-cold Buffer A containing 10 m*M* HEPES (pH 7.4), 1 m*M* EDTA, 1 m*M* EGTA, 0.34 *M* sucrose, 10% glycerol, 10 μg/ml leupeptin, 10 μg/ml aprotinin, 1 m*M* benzamidine, and 1 m*M* phenylmethylsulfonyl fluoride. Cell lysates were centrifuged at 16,000 *g* for 5 mins and then the supernatant was centrifuged at 100,000 *g* at 4°C for 45 mins to separate membrane and cytosolic fractions. The supernatant was considered the cytosolic fraction. The pellet was resuspended with Buffer B, which is Buffer A with 1% Triton X-100, and was then placed on ice for 1 hr; the suspension was gently mixed several times. The suspension was centrifuged at 16,000 *g* at 4°C for 10 mins; the supernatant contained the solubilized membrane fraction. Proteins in each fraction were analyzed by Western blot as described above.

PKC Kinase Assay. PKC activity was determined by measuring ^{32}P incorporation from [γ-^{32}P]ATP into a synthetic PKC substrate peptide, a fragment of glycogen synthase (GS) (Sigma Chemical), according to the procedures previously described (31–33). Cytosolic and membrane fractions of cells were isolated by procedures described in the "PKC Translocation Assay" section, above. PKC activity was calculated as the difference between ^{32}P incorporated into the GS substrate peptide in the presence of $CaCl_2$-phosphatidylserine and EGTA. Results were expressed as picomoles of ^{32}P incorporated per milligram of protein per minute ($pmol \cdot mg^{-1} \cdot min^{-1}$).

Activated Ras Activity Assay. Activated Ras was detected by an affinity pull-down assay with GST-Raf-1 agrose (EZ-Ras-Detect kit; Pierce Biotechnology), used according to the manufacturer's instructions. U373MG cells transfected with vector H-Ras wild-type active cDNA or H-Ras dominant negative cDNA were exposed to ET-1 (100 n*M*) for 5 mins, or serum-starved untransfected U373MG cells were exposed to ET-1 (100 n*M*) for 2–30 mins. Cells were washed with 1 ml ice-cold PBS and lysed in 500 μl Lysis-Binding-Wash (LBW) buffer. Five hundred micrograms of fresh cell lysate was incubated with 30 μg GST-Raf-1 binding domain (RBD) agarose in a spin column for 1 hr at 4°C with gentle rotation. The agarose beads were washed four times with LBW buffer, and 50 μl of sample buffer was added and the solution boiled for 5 mins. After a brief spin, supernatants were collected and applied to 12% SDS-PAGE. The proteins were transferred from gels to nitrocellulose membranes and probed with monoclonal anti-Ras (1:200, provided with kit). A horseradish peroxidase–conjugated anti-mouse IgG antibody was used as secondary antibody, and the ECL reagents were used for immunoblotting detection.

Calcium Imaging. Intracellular Ca^{2+} ($[Ca^{2+}]_i$) release was determined by calcium imaging (by ratiometric technique using Fura-2 AM), as previously described (34). U373MG cells were seeded on the cover slip in a 35-mm dish and grown for 24 hrs. On the following day, cells were washed with a modified Krebs-Ringer buffer solution (KRB; 115 m*M* NaCl, 2.5 m*M* $CaCl_2$, 1.2 m*M* $MgCl_2$, 24 m*M* $NaHCO_3$, 5 m*M* KCl, 5 m*M* glucose, and 25 m*M* HEPES [pH 7.4]) and incubated with 3 μ*M* Fura-2 AM (Molecular Probes) for 30 mins at 37°C. Fura-2 fluorescence from these cells was monitored at 37°C by the ratio technique (excitation at 340 and 380 nm, emission at 500 nm) under a Nikon Diaphot microscope using Metafluor software (Universal Imaging, West Chester, PA). $[Ca^{2+}]_i$ was calculated according to the formula provided by Grynkiewicz *et al*. (35). Calibrations were performed *in vivo*, and conditions of high $[Ca^{2+}]_i$ were achieved by adding the Ca^{2+} ionophore 4-Bromo-A23187 (3 μ*M*; Calbiochem), whereas conditions of low $[Ca^{2+}]_i$ were obtained by adding EGTA (5 μ*M*). $[Ca^{2+}]_i$ for each treatment was measured in at least eight different cells and in two cover slips.

Results

ET-1–Induced Cell Proliferation of U373MG Astrocytoma Cells and Phosphorylation of ERK1/2. Previous observations demonstrated that 100-n*M* ET-1 treatment for 24 hrs increased U373MG astrocytoma cell proliferation using both [^{3}H]thymidine incorporation and formazan-MTT assays (7). In the present series of experiments, the role of ERK1/2 in ET-1–induced cell proliferation was determined using a similar ET-1 dosing. The [^{3}H]thymidine incorporation assay was employed to investigate ET-1–induced cell proliferation in the absence or presence of inhibitors of several

signaling pathways (Fig. 1A). ET-1 induced a 25%–30% increase in cell proliferation ($n = 3$), whereas 10 μ*M* U0126 (an inhibitor of MEK1/2), 2 μ*M* chelerythrine (an inhibitor of PKC), and 25 μ*M* LY294002 (an inhibitor of PI3K) completely blocked ET-1–induced cell proliferation; 5 μ*M* genistein (an inhibitor of protein tyrosine kinases [PTKs]) had no effect.

A formazan-MTT assay was also employed to measure cell proliferation in the presence of inhibitors of signaling pathways. U373MG astrocytoma cells were seeded in 96-well plates and treated with 100 n*M* U0126 (inhibitor of MEK1/2) and 5 μ*M* PD98059 (inhibitor of MEK1) with and without 100 n*M* ET-1. Cell proliferation was significantly stimulated by ET-1 in U373MG ($P < 0.05$), by 170%, after 24 hrs of treatment, and this effect was completely blocked by U0126, even at a low concentration (100 n*M*), whereas it was only partially blocked by 5 μ*M* PD98059 (Fig. 1B). Although the trend of inhibition of cell proliferation by drugs was similar in both assays, there were some differences between the assays. The lower basal levels of cell proliferation in treatments with drugs than those in controls were seen in the thymidine incorporation assay, whereas the basal levels in the drug-treated groups were almost the same as those in the control group of the formazan-MTT assay. In the thymidine incorporation assay the cells were treated with drugs for 24 hrs, whereas [^{3}H]thymidine was added 8 hrs before the cells were harvested. Therefore, the cell proliferation in the drug-treated group had been inhibited for 16 hrs before [^{3}H]thymidine was added: thus, the lower uptake of thymidine into cells treated with drugs compared to the control. Such an effect can explain the lower basal levels detected in the thymidine incorporation assay.

ERK1/2, the key element of the MAPK pathway, was phosphorylated by 100 n*M* ET-1 in a time-dependent manner (Fig. 1C). The phosphorylation of ERK1/2 reached the highest level after a 5-min treatment with ET-1 and subsequently returned to basal level after 30 mins. PD98059 at 25 μ*M* partially blocked the phosphorylation induced by ET-1; it also attenuated the basal level of ERK1/2 phosphorylation (Fig. 1D). Both basal and ET-1–induced phosphorylation of ERK1/2 were completely blocked by 10 μ*M* U0126 (Fig. 1E).

ET-1–Induced Phosphorylation of ERK1/2 Occurs Through ET_B Receptors. Although the ET_B receptor is predominantly expressed in U373MG cells (36), it was important to determine which receptor was responsible for ERK1/2 phosphorylation induced by ET-1. To address this question, selective ET-receptor antagonists BQ610 (ET_A antagonist) and BQ788 (ET_B antagonist) were used. These compounds were used at 2 μ*M* and were administered to U373MG cells for 30 mins before ET-1 treatment. BQ788 ($IC_{50} = 1.2$ n*M*) completely blocked the ERK1/2 phosphorylation induced by ET-1, whereas BQ610 ($IC_{50} = 20$ n*M*) had no effect (Fig. 2). This result is also consistent with the binding assay results in which the ET_B receptor antagonist BQ788 completely blocked [^{125}I]–ET-1 binding in U373MG astrocytoma cells, whereas the ET_A receptor antagonist BQ610 and FR139317 did not (36).

Involvement of PKC Is Necessary for Proliferation of U373MG but Is Not Necessary for Phosphorylation of ERK1/2 Induced by ET-1. To test the role of PKCs in ET-1–induced cell proliferation of U373MG astrocytoma cells, 2 μ*M* chelerythrine and 1 μ*M* RO-31–8425, general inhibitors of PKCs, were employed. Blockage of PKC activity by chelerythrine and RO-31–8425 inhibited ET-1–induced proliferation of U373MG cells (Figs. 1A and 3A). Both MAPK-ERK and PKCs were found to be involved in the ET-1–induced cell proliferation of U373MG astrocytoma cells. However, it is well known that PKC activation can result in MAPK-ERK activation; therefore, the question was whether these pathways exerted their effects in a parallel pattern or whether there was a direct interaction or "cross talk" between them. To address this question, the effects of PKC inhibitors on ERK1/2 phosphorylation were determined. PMA, the phorbol ester known to activate PKCs, was administered (1 μ*M*) in U373MG cells for 30 mins and it induced a strong phosphorylation of ERK1/2 (Fig. 3B). However, the application of either 2 μ*M* chelerythrine or 1 μ*M* RO-31–8425 did not abolish the ERK1/2 phosphorylation induced by ET-1 (Fig. 3B).

ET-1 Did Not Activate Conventional and/or Novel PKC (c/nPKC) Isoforms. Our results have shown that PKCs are involved in the ET-1–induced cell proliferation of U373MG astrocytoma, but not in ET-1–induced ERK1/2 phosphorylation. To identify the isoforms of PKCs involved in cell proliferation, we measured the phosphorylation of PKC and the translocation of PKC from cytosol to membranes both by Western blot and using a PKC kinase assay. In the PKC kinase assay, ET-1 treatment for 5 mins in U373MG cells did not activate the c/nPKCs, whereas 1-μ*M* PMA treatment increased the activities of PKCs, which resulted in PKC phosphorylation and translocation from cytosol to membrane (Fig. 4A and B). Furthermore, the results from the kinase assay also showed that blockade of MEK1/2 by U0126 did not affect the activation and translocation of PKCs. Therefore, MEK1/2 and ERK1/2 did not directly activate PKCs in U373MG astrocytoma. Phosphorylation of PKCs in cytosolic and membrane fractions was also determined by Western blot using anti–phospho-pan-PKC antibody, which can recognize phosphorylated PKC-α, βI, βII, δ, η, θ, and ε (Fig. 4C). SDS-PAGE gels stained with Coomassie blue were used as loading controls. ET treatment of U373MG cells treated from 1 to 10 mins did not alter the pattern of phosphorylation and translocation of PKC-α, βI, βII, δ, and ε either in cytosolic or membrane fractions (Fig. 4C). In positive controls, after a 30-min treatment with 1 μ*M* PMA, these phosphorylated isoforms of PKC, shown as four bands in the blot, were translocated to membrane, whereas 1 μ*M* PMM, which is an inactive analog of PMA, did not activate PKC. Because this anti–phospho-pan-PKC antibody can

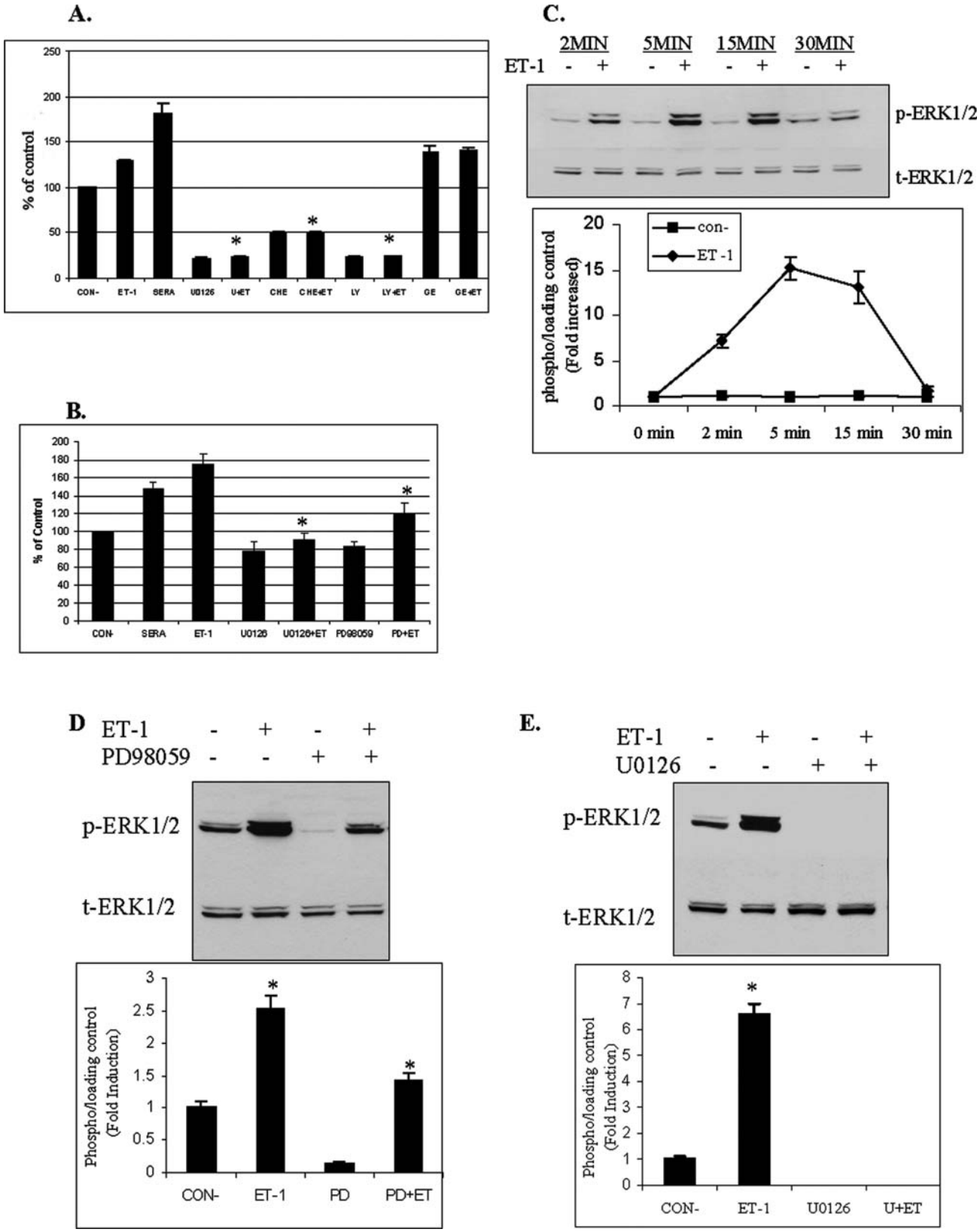

Figure 1. Cell proliferation of U373MG cells was blocked by inhibition of phosphorylation of ERK1/2 induced by ET-1. (A) Cell proliferation of U373MG cells was determined using a [^{3}H]thymidine incorporation assay 24 hrs after U373MG cells were pretreated with 10 μM U0126 (a MEK1/2 inhibitor), 2 μM chelerythrine (CHE, a PKC inhibitor), 25 μM LY294002 (LY, a PI3K inhibitor), and 5 μM genistein (GE, a PTK inhibitor) 30 mins before being treated with 100 nM ET-1. * $P < 0.05$ vs. ET-1 treatment alone; one-way analysis of variance (ANOVA)/Student-Newman-Keuls (SNK) test. (B) Cell proliferation of U373MG cells was determined by formazan-MTT assay 24 hrs after U373MG cells were pretreated

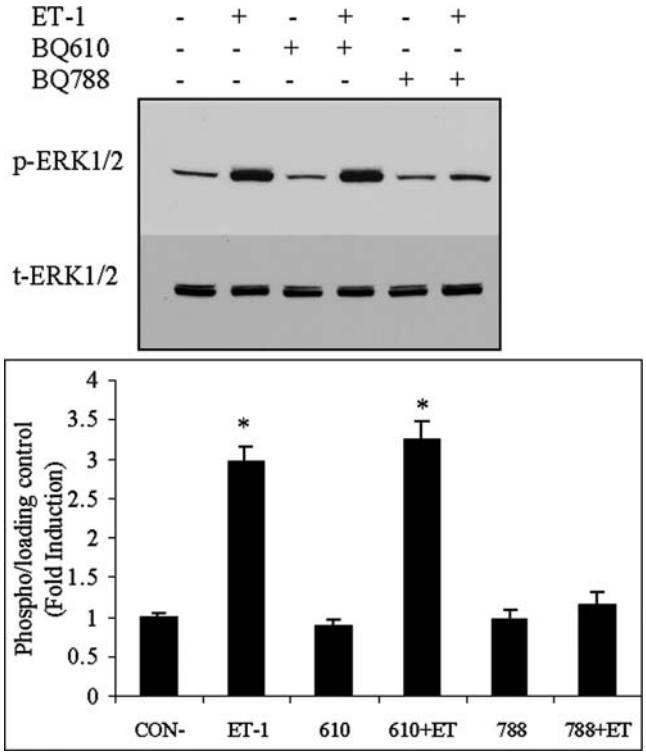

Figure 2. ET-1–induced phosphorylation of ERK1/2 occurred through ET_B receptors. Western blot shows phosphorylation of ERK1/2 induced by ET-1 after U373MG astrocytoma cells were pretreated with BQ610 (2 μM) and BQ788 (2 μM) for 30 mins followed by an application of 100 nM ET-1 for 5 mins. The data shown are from a representative sample from three individual experiments. * $P < 0.05$ ET-1 treatment versus relative control; one-way ANOVA/SNK test.

recognize both conventional PKCs (α, βI, βII) and novel PKCs (δ, η, θ, and ε), it was concluded that ET-1 did not activate c/nPKCs.

ET-1 Did Not Elevate the $[Ca^{2+}]_i$ Mobilization and IP_3 Generation. The current data indicated that ET-1 did not activate c/nPKC isoforms, but we still needed to investigate whether ET-1 treatment increases $[Ca^{2+}]_i$ levels, which could activate cPKCs. Fura-2 calcium imaging was used to monitor the concentration of $[Ca^{2+}]_i$. After ET-1 was applied to U373MG cells, the ratio at 340 nm to 380 nm did not change (Fig. 5A), whereas carbachol, an agonist of acetylcholine receptors, increased the 340:380 ratio slightly. Treatment with A23187, a calcium ionophore reagent, increased $[Ca^{2+}]_i$ rapidly. To further confirm that IP_3-induced $[Ca^{2+}]_i$ and DAG signaling were not involved in ET-1–induced PKC activation and ERK1/2 activation, astrocytoma cells were treated with U73122 (a phospholipase C inhibitor). U73122 did not attenuate the ERK1/2

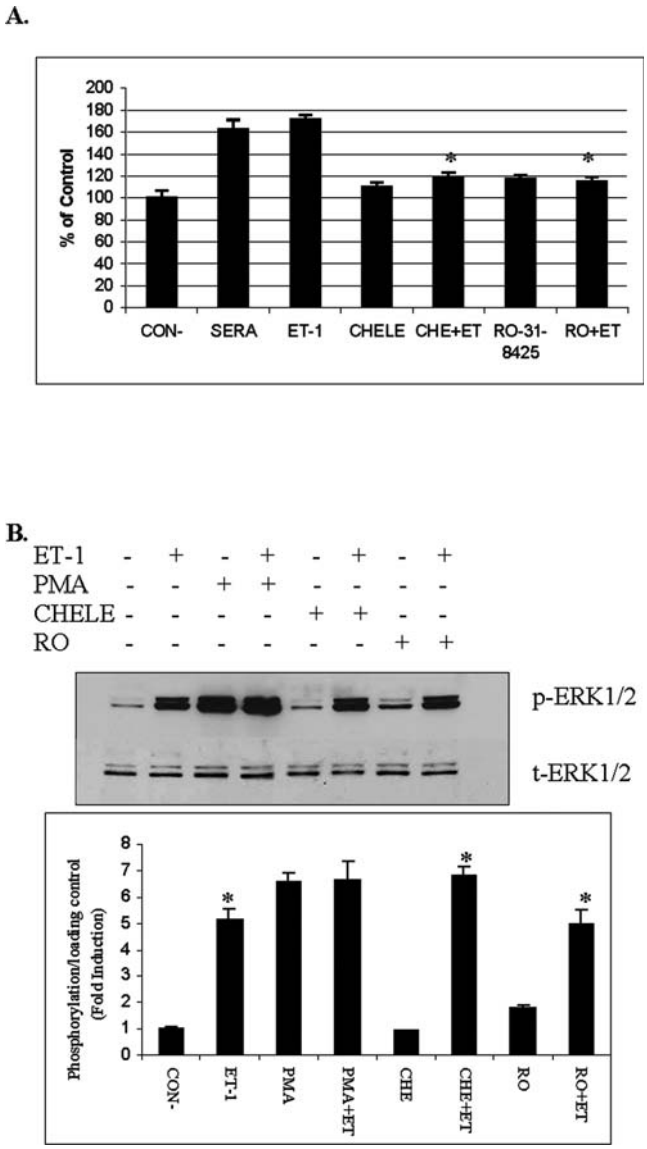

Figure 3. Involvement of PKC is necessary for proliferation of U373MG cells; however, phosphorylation of ERK1/2 induced by ET-1 is PKC independent. (A) Cell proliferation of U373MG cells was determined by formazan-MTT assay 24 hrs after U373MG cells were treated with 2 μM chelerythrine (CHE, a PKC inhibitor). * $P < 0.05$ versus ET-1; one-way ANOVA/SNK test. (B) U373MG cells were pretreated with 1 μM PMA, 2 μM chelerythrine, and 1 μM RO-31–8425 (RO) followed by application of ET-1 for 5 mins. Western blot was employed to detect the phosphorylation of ERK1/2 in total cell lysate. The data shown are from a representative sample from three individual experiments. * $P < 0.05$ ET-1 treatment versus relative control; one-way ANOVA/SNK test.

←
with 100 nM U0126 (a MEK1/2 inhibitor) and 5 μM PD98059 (a MEK1 inhibitor) 30 mins before being treated with 100 nM ET-1. * $P < 0.05$ vs. ET-1 treatment alone; one-way ANOVA/SNK test. (C) Western blot is employed to detect the phosphorylation of ERK1/2 induced by ET-1 over several time points after U373MG cells were treated with 100 nM ET-1 from 2 mins to 30 mins. (D, E) Western blot indicates phosphorylation of ERK1/2 induced by ET-1 after cells were pretreated with PD98059 (25 μM) and U0126 (10 μM) for 30 mins followed by application 100 nM ET-1 for 5 mins. The data shown are from a representative sample from three individual experiments. * $P < 0.05$ ET-1 treatment vs. relative control; one-way ANOVA/SNK test (for C, D, and E).

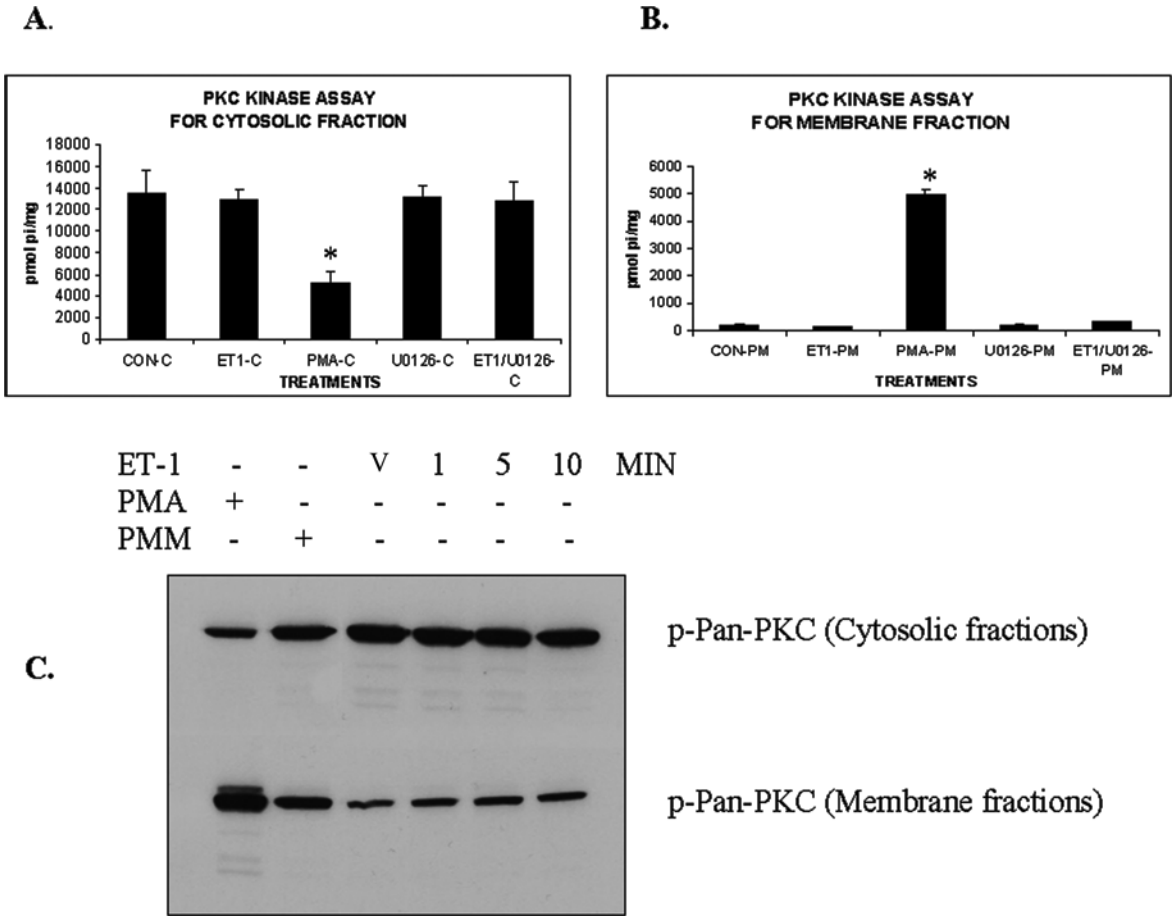

Figure 4. ET-1 did not activate conventional and novel (c/n) PKC isoforms in U373MG cells. (A, B) Activities of c/nPKC were determined by kinase assay that used a PKC substrate phosphorylated by cytosolic and membrane fraction in the presence of Ca^{2+} and DAG. * $P < 0.05$ PMA treatment versus relative control; one-way ANOVA/SNK test. (C) Phosphorylation and translocation of c/nPKC isoforms were detected by Western blot for cytosolic and membrane fractions isolated from U373MG cells that were pretreated with 1 μM PMA (positive control), 1 μM PMM (negative control), and DMSO (vehicle, labeled as "V") for 30 mins followed by an application of 100 nM ET-1 for 1 min to 10 mins. The data shown are from a representative sample from three individual experiments.

phosphorylation induced by ET-1 (Fig. 5B). The results indicated that ET-1 did not promote the calcium release in U373MG cells and that there was no cross talk between PKC and ERK1/2 pathways. These findings were also consistent with the result that ET-1 did not activate c/nPKCs in U373MG cells and could activate atypical PKCs, since chelerythrine, a PKC inhibitor, blocked ET-1–induced cell proliferation.

Inhibition of H-Ras Does Not Block ERK1/2 Phosphorylation Induced by ET-1. Ras, a member of the small GTPase family, is considered an upstream element involved in the activation of ERK1/2 in mammalian cell types (22, 37, 38), including COS cells (39), Jurkat T cells (40), and astrocytes (41). To identify the role of Ras in the signaling pathway induced by ET-1, pharmacologic and molecular biological approaches were used. First, a GST pulldown assay was used to detect Ras activities after ET treatment at different time points. Only the active GTP-bound Ras is pulled down by the GST-RBD agarose. At 2 and 5 mins post–ET treatment, the active form of Ras increased and began to decline after 15 mins of ET treatment (Fig. 6A). U373MG cells were also pretreated for 30 mins with FTI-277 (10 μM), which is a selective inhibitor of H-Ras, a member of the Ras family (42, 43), followed by an application of 100 nM ET-1 for 5 mins. Surprisingly, ET-1–induced phosphorylation of ERK1/2 was not blocked by FTI-277 (Fig. 6B).

In another set of experiments, both ERK1/2 phosphorylation and Ras activity were assessed following ET-1 treatment of U373MG cells transfected with wild-type, active, and dominant negative H-Ras plasmid cDNAs. U373MG cells were transfected with active H-Ras and dominant negative H-Ras S17N plasmid cDNA for 36 hrs; this step was followed by an application of ET-1 for 5 mins. Phosphorylation of ERK1/2 was greatly amplified by overexpression of active wild-type H-Ras, with and without ET-1. Treatment with ET-1 enhanced this phosphorylation (Fig. 6C). However, introduction of a dominant negative of H-Ras did not abolish the ET-1–induced phosphorylation of ERK1/2 as compared with controls, which were transfected

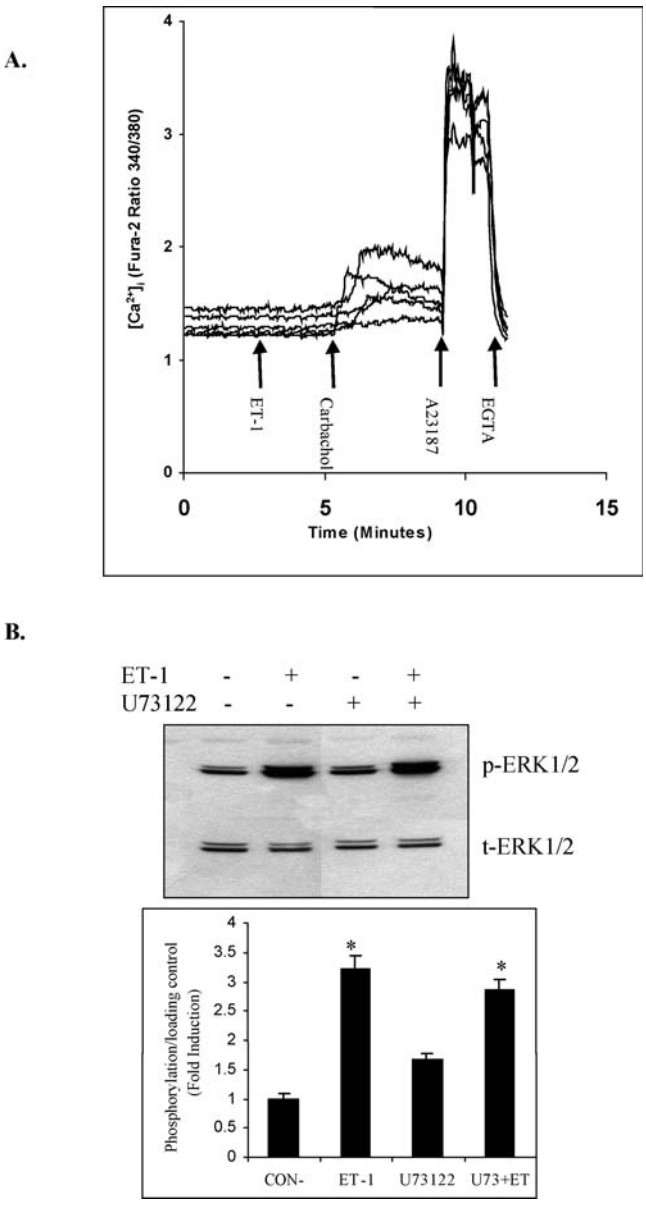

Figure 5. Intracellular Ca^{2+} was not changed after U373MG cells were treated with 100 n*M* ET-1, and blockage of IP3 generation did not block the phosphorylation of ERK1/2 induced by ET-1. (A) Concentration of intracellular Ca^{2+} in U373MG cells was monitored by Fura-2 calcium imaging. U373MG cells cultured on cover slips were treated with 100 n*M* ET-1, 100 μ*M* carbachol, AG23187, and EGTA after preincubation with Fura-2 for 30 mins ($n = 8$). (B) U373MG cells were pretreated with 2 μ*M* U-73122, followed by an application of ET-1 for 5 mins. Western blot was employed to detect the phosphorylation of ERK1/2 in total cell lysate. * $P < 0.05$ ET-1 treatment versus relative control; one-way ANOVA/SNK test.

with the pcDNA3 vector. Activity of Ras was also determined in U373MG cells transfected with H-Ras cDNA and H-Ras S17N dominant negative cDNA. In U373MG cells transfected with active wild-type Ras, the activity of Ras was increased significantly by overexpression of H-Ras (Fig. 6D). This elevated activity, a reflection of H-Ras overexpression, was blocked partially by application of FTI-277 (Fig. 6D). It is therefore likely that a Ras unlike H-Ras may be involved in ET-1–mediated ERK1/2 phosphorylation in U373MG astrocytoma cells.

ET-1–Induced Phosphorylation of ERK1/2 Was Not Blocked by Inhibition of Either PTK or Transactivation of Receptor Tyrosine Kinase. Some studies reported that activation of Ras-Raf-MAPK pathway by ET-1 occurs through the PTKs such as focal adhesion kinase (FAK), c-Src, etc. (26, 44, 45). We also considered that PTKs might be part of the upstream elements and might play an important role in activating a similar signaling induced by ET-1 in U373MG astrocytoma cells. Genistein (5 μ*M*), an inhibitor of PTKs, did not block either ET-1–induced cell proliferation (Fig. 1A) or ET-1–induced phosphorylation of ERK1/2 (Fig. 7A). To further identify other potential PTKs involved in the ET-1–induced signaling, the inhibitors of intracellular tyrosine kinases, such as AG82 and herbimycin A, were used to attenuate the kinase activity of p125FAK and p60 c-Src, as well as other PTKs. Neither the co-administration of AG82 (10 μ*M*) and herbimycin A (1 μ*M*) nor the administration of AG82 alone decreased ET-1–induced phosphorylation of ERK1/2 (Fig. 7B). Although previous reports in other cell types demonstrated that the ET-1–triggered Ras-Raf-MAPK pathway occurs through PTKs such as FAK, c-Src, etc., such a mechanism does not appear to be involved in ET-1–induced triggering of the Ras-Raf-MAPK in U373MG astrocytoma cells.

However, it has also been reported that ET-1, through its ET receptors, can transactivate the EGF receptor by which ERK1/2 is phosphorylated and activated through the Ras-Raf-MAPK pathway. This was shown in rat mesangial cells (46), human vascular smooth muscle cells (47, 48), human melanocytes (49), and human ovarian carcinoma cells (50). Therefore, AG1478, an inhibitor of the EGF receptor tyrosine kinase, was used to examine ET-1 effects on receptor tyrosine kinases. AG14781 (1 μ*M*) inhibited EGF-induced phosphorylation of ERK1/2 completely, but did not block ET-1–induced phosphorylation of ERK1/2 (Fig. 7C). Additionally, EGF (10 ng/ml) was used as a positive control, and its effects on ERK1/2 were blocked by AG1478 (1 μ*M*) (Fig. 7C). EGF-induced phosphorylation of ERK1/2 by activation of the EGF receptor tyrosine kinase was completely blocked by application AG1478, an inhibitor of the EGF receptor tyrosine kinase. However, AG1478 did not inhibit the effects of ET-1 on activation of MAPK or phosphorylation of ERK1/2. Therefore, in U373MG astrocytoma cells, there is no transactivation of the EGF receptor tyrosine kinase by ET-1 receptors, and, consequently, ET-1 does not play a role in ERK1/2 activation.

PI3K Is Involved in ET-1–Induced Cell Proliferation in U373MG Cells, but ET-1–Induced Phosphorylation of ERK1/2 Is Independent of PKC and PI3K. The PI3K-Akt pathway has been implicated in the signaling pathways leading to cell proliferation (51, 52). It was reported that the βγ subunit of activated G proteins of GPCRs activates PI3K and subsequently leads to activated

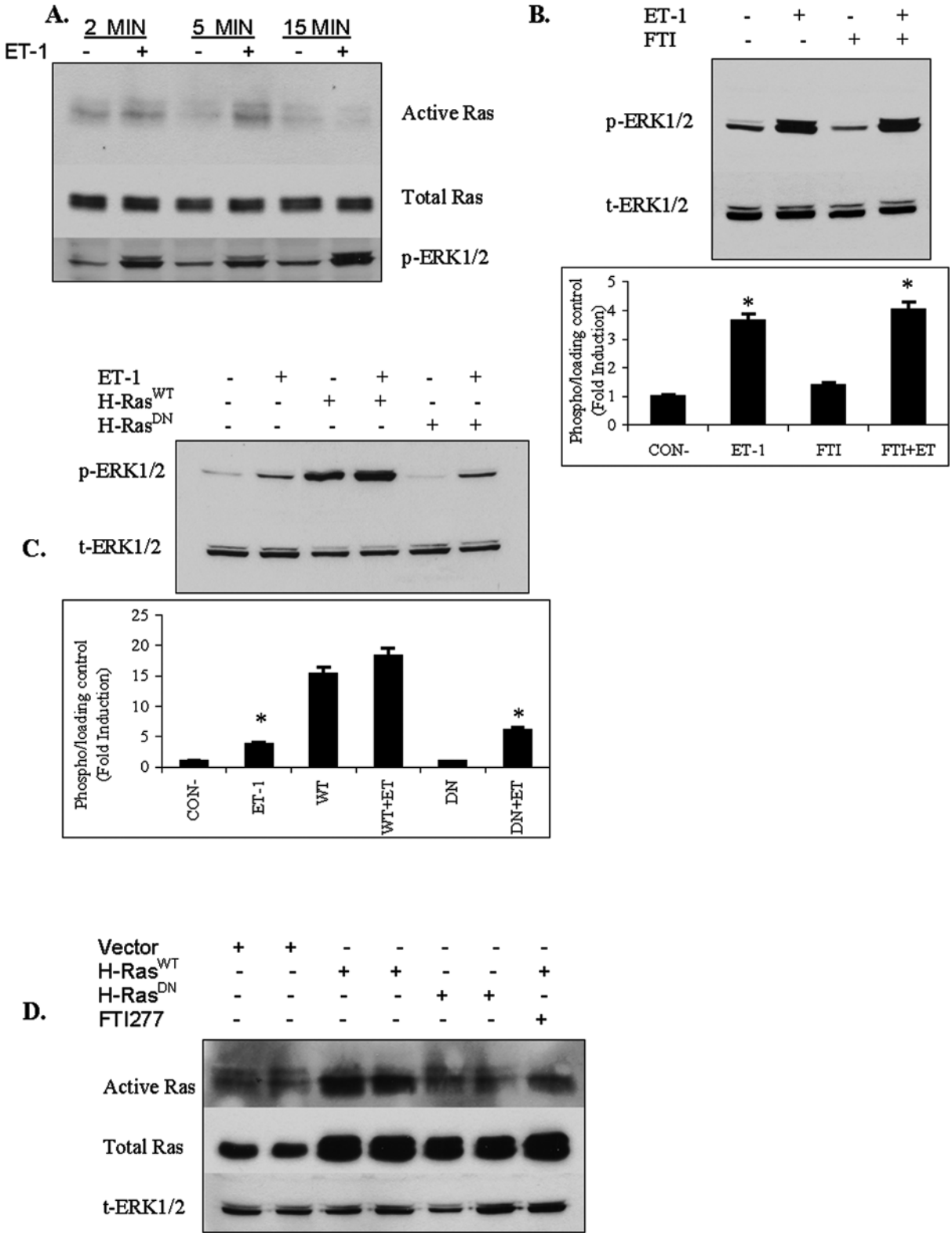

Figure 6. Inhibition of H-Ras does not block the phosphorylation of ERK1/2 induced by ET-1, even though ET-1 activates Ras. (A) GST-pulldown assay was used to detect Ras activity after cells were treated with 100 n*M* ET-1 for different time points. (B) Phosphorylation of ERK1/2 induced by ET-1 was determined by Western blot after cells were pretreated with FTI-277 (FTI, 10 μM), an inhibitor of Ras, for 30 mins followed by an application of 100 n*M* ET-1 for 5 mins. (C) Western blot was employed to detect phosphorylation of ERK1/2 induced by ET-1 after U373MG cells were transfected with 10 μg vector, wild-type H-Ras (WT) and dominant negative H-Ras (DN) cDNA for 24 hrs followed by an application of 100 n*M* ET-1 for 5 mins. (D) GST-pulldown assay was used to detect Ras activity after U373MG cells were transfected with 10 μg vector, wild-type H-Ras and dominant negative H-Ras cDNA for 24 hrs followed by an application of 100 n*M* ET-1 for 5 mins. The data shown are from a representative sample from two individual experiments. * $P < 0.05$ ET-1 treatment versus relative control; one-way ANOVA/SNK test.

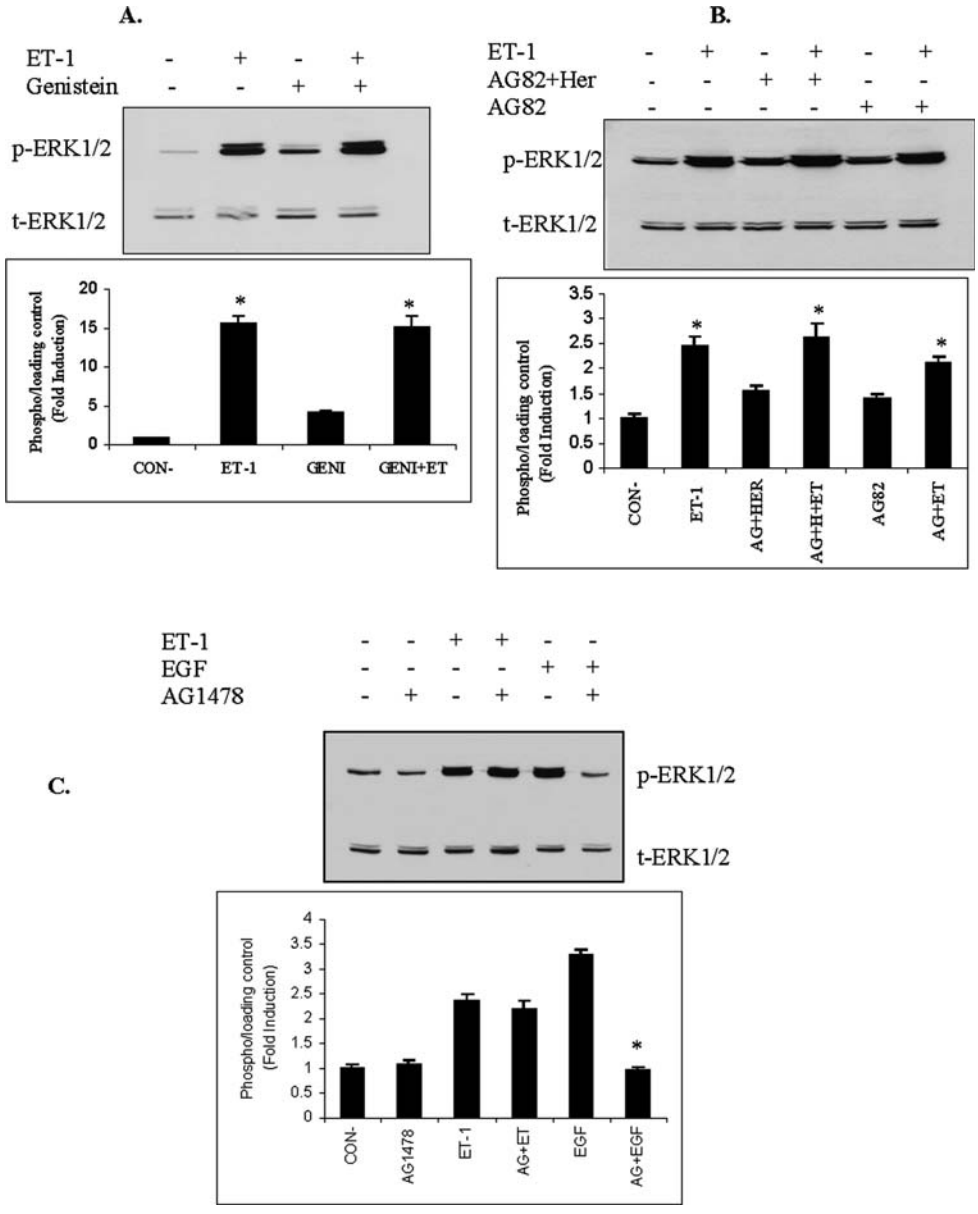

Figure 7. Inhibition of protein tyrosine kinases did not block the phosphorylation of ERK1/2 induced by ET-1. Also, ET-1 did not transactivate EGF receptor tyrosine kinase. (A) U373MG cells were pretreated with 5 μM genistein (GENI), an inhibitor of protein tyrosine kinase, followed by an application of ET-1 for 5 mins. Western blot was employed to detect the phosphorylation of ERK1/2 in total cell lysate. (B) 10 μM AG82 (AG) and/or 1 μM herbimycin A (HER) were used to pretreat U373MG cells for 30 mins, followed a 5-min ET-1 treatment. (C) Genistein and 1 μM AG1478 (an inhibitor of EGF receptor tyrosine kinase) were used to pretreat U373MG cells for 30 mins, followed a 5-min ET-1 or EGF (10 ng/ml) treatment. The data shown are from a representative sample from three individual experiments. * $P < 0.05$ ET-1 treatment versus relative control; one-way ANOVA/SNK test.

PKB/Akt (53–55). The role of the PI3K pathway in ET-1–induced U373MG astrocytomas cell proliferation is unknown; therefore, the effect of the PI3K on ET-1–induced cell proliferation was examined using formazan and [^{3}H]-thymidine incorporation assays. Inhibition of PI3 kinase by 25 μM LY294002 completely blocked the ET-1 mitogenic effects in U373MG cells (Figs. 1A and 8A). Based on this finding, Akt activation was assessed. A 5-min ET-1 treatment significantly promoted the phosphorylation of Akt as well as phosphorylation of ERK1/2. The ET-1–induced phosphorylation of Akt was blocked completely by LY294002, but not by chelerythrine, whereas the phosphorylation of ERK1/2 was not blocked by either of these two compounds (Fig. 8B). Phosphorylation of ERK1/2 by ET-1 appears to be PKC and PI3K independent; albeit, activation of PI3K and AKT occurs.

Discussion

In the current study, several findings were made that were reflective of ET-1's mitogenic potential in U373MG astrocytoma cells. It was determined that three signaling pathways, including ERK1/2, PKC, and PI3K, were

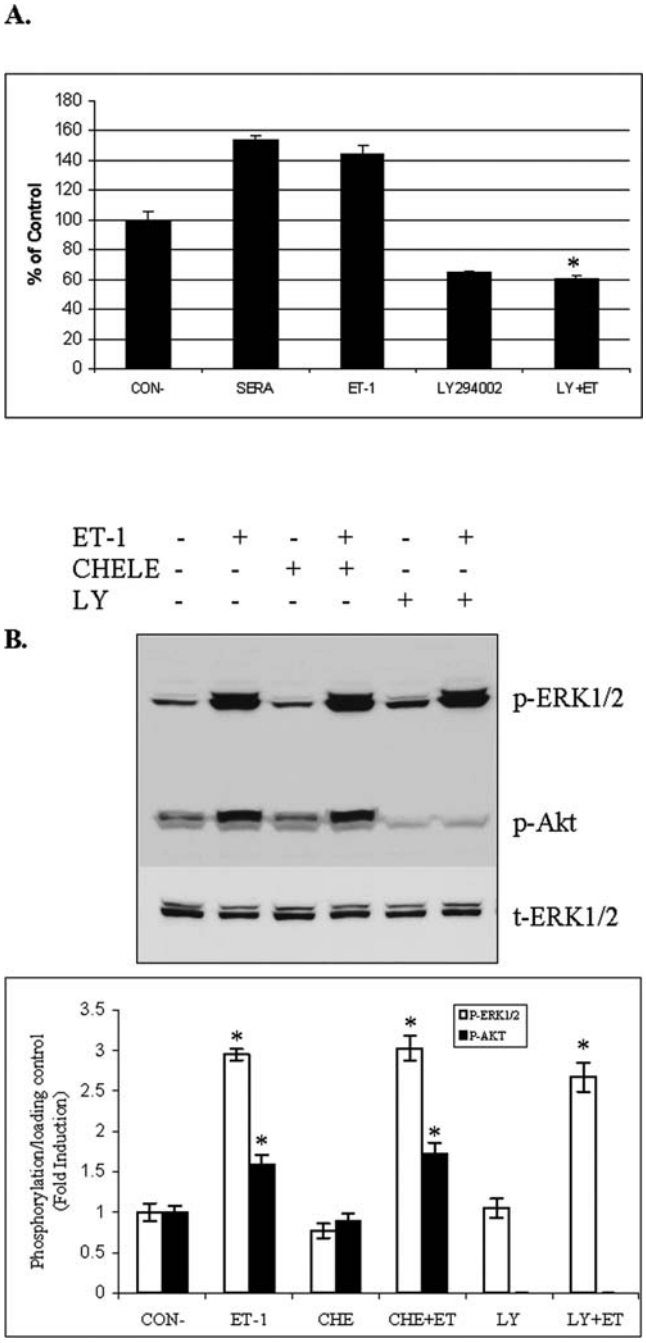

Figure 8. Inhibition of PI3K by LY294002 abolished cell proliferation of U373MG cells stimulated by ET-1, and ERK1/2 phosphorylation induced by ET-1 is PKC and PI3K independent. (A) Cell proliferation of U373MG cells was determined by formazan-MTT assay 24 hrs after U373MG cells were treated with 25 μM LY294002 (LY). * $P <$ 0.05 versus ET-1; one-way ANOVA/SNK test. (B) U373MG cells were pretreated with 2 μM chelerythrine (CHE) and 25 μM LY294002 followed by an application of ET-1 for 5 mins. Western blot was employed to detect the phosphorylation of ERK1/2 and Akt in total cell lysate. The data shown are from a representative sample from three individual experiments. * $P < 0.05$ ET-1 treatment versus relative control; one-way ANOVA/SNK test.

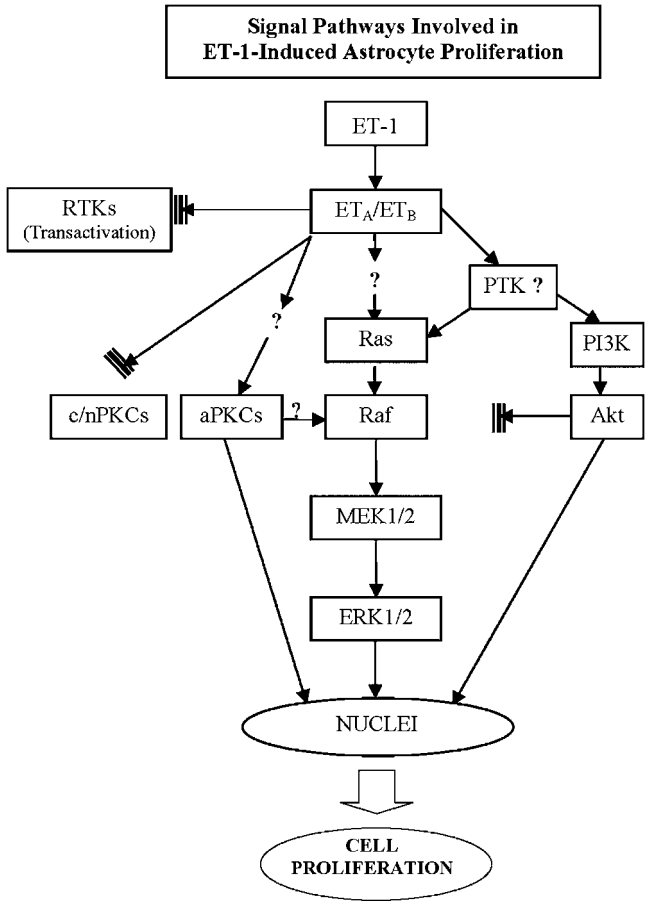

Figure 9. Possible signaling pathways involved in ET-1–induced U373MG astrocytoma cell proliferation. ERK-MAPK, PKC, and PI3K pathways are involved in ET-1–induced cell proliferation in U373MG astrocytoma. Blockade of one of these three pathways will completely abolish the cell proliferation induced by ET-1. No direct cross talk among these pathways is found in this cell type. Some of well-identified protein tyrosine kinases, including c-Src and FAK, are not involved in this event, and transactivation of EGF receptor by ET-1 through $ET_{A/B}$ receptors is not found in this cell line.

activated by ET-1 within a short period of time (i.e., within 5 mins). The combined consequence of activating these three pathways resulted in U373MG cell proliferation. It appeared that ERK1/2 activation was involved but was independent of PKC and PI3K activation by ET-1. It was also determined that the ET_B receptor was the dominant receptor involved in ERK1/2 phosphorylation and in increased cell proliferation. Although Ras appears to be a signaling pathway involved in activation of the ERK-MAPK pathway by ET-1, H-Ras was not, indicating that some other Ras members may be involved. It was also shown that some general PTKs, including c-Src, FAK, etc., are not involved in ET-1 stimulation in U373MG cells, as has been reported in other cell types (23, 26, 44, 45, 56). In addition, ERK1/2 phosphorylation was not transactivated by the EGF receptor by ET-1.

ET-1 induces cell proliferation in many types of cells *via* its ET_A and ET_B receptors, and although diverse

signaling pathways coupled to ET-1 receptors have been identified, the precise mechanisms by which ET-1 stimulates cell proliferation in astrocytes remain unclear. Our present study has shown that ET-1 is a mitogen for U373MG astrocytoma cells, a result that is similar to that seen in earlier studies in human optic nerve head astrocytes (7); our study has also shown that the cell proliferation of U373MG cells induced by ET-1 is MAPK-ERK, PKC, and PI3K dependent. Blockade of one of these three parallel pathways will inhibit the mitogenic effects of ET-1 in U373MG astrocytoma cells. This result may arise from activation of the key components (e.g., common and discrete transcription factors) in the proliferation response. These key components could be downstream kinases of these initial signaling pathways or they could be selective transcriptional factors in which these signaling pathways converge. The phosphorylation of ERK1/2 is a key step in triggering downstream signalings and potential activation of transcriptional factors, such as c-Myc, Elk-1, c-Fos, etc. (41, 57). PKC and PI3K are also involved in ET-1–mediated activation of transcription factors (41, 58–60). It has been suggested that some transcription factors, such Elk-1, c-Fos, and AP-1, are controlled simultaneously by MAPK-ERK and PKC (41, 61, 62), whereas p38 and JNK share different transcription factors. Some other downstream kinases, including Rsk and p70S6K, are also under control of these three pathways. We propose that blockage of any one of the upstream pathways will completely abolish the activation of downstream kinases or transcription factors dependent on these signals of activation.

Mitogenic effects have been shown to be a characteristic of ET's effects on tumor cells. There are several reports showing that ET-1 is a survival factor for many different blastomas, including T98G glioblastoma (4). Naidoo *et al*. (3) showed a significant distribution of ET-1 mRNA by *in situ* hybridization in human brain autopsy samples and astrocytic tumors, which is indicative of ET's role in tumor progression. In another report, four human glioblastoma cell lines were found to express all components of ET-1 including endothelin converting enzyme and $ET_{A/B}$ receptors; it was also determined that Bosentan (an $ET_{A/B}$ antagonist) induced apoptosis in these cell lines (5). Furthermore, in one cell line, LNZ308, Bosentan inhibited FLICE/Caspase-8 inhibitory protein, promoting cell survival (5). In the same study, it was reported that ET-1 induced ERK1/2 phosphorylation but did not promote cell proliferation of LNZ308 glioblastoma cells (5). However, in the present study involving U373MG cells, ET-1 did activate ERK1/2, and this activation resulted in increased cell proliferation as well.

ET-1 has been shown to promote proteolytic activity in ovarian carcinomas, typically *via* ET_A receptor activation, causing an increase in both expression and activity of MMP-2, MMP-9, urokinase-type plasminogen activator, PAI-1, and PAI-2 (63). This finding indicates that multiple signaling cascades are necessary to activate various aspects of tumor progression, including proliferation, migration, and invasion. Furthermore, ET-1–induced phosphorylation of ERK1/2 was inhibited by BQ788, a selective antagonist of the ET_B receptor, indicating that ET-1–induced activation of the MAPK pathway occurred through activation of the ET_B receptor. In T98G glioblastomas, treatment with an ET_A antagonist caused significant cell death, whereas treatment with an ET_B antagonist had no such effect (4). The ET_B receptor is predominant in the CNS (17). In the normal rat spinal cord, there is ET_A immunoreactivity in the vascular system and afferent nerve fibers, whereas there is broad ET_B immunoreactivity in gray and white matter (19). In response to spinal cord injury the expression of ET_B was increased, resulting in hypertrophy of astrocytes. In the optic nerve crush model, there is increased expression of GFAP and ET_B, which is abolished by an application of the $ET_{A/B}$ inhibitor Bosentan (18). We previously reported that the ET_B receptor and GFAP expression are increased and co-localized at the optic nerve head in rats that had their intraocular pressure elevated; moreover, the immunoreactivity of ET-1 was also elevated at the same sites (6). The results from both cell culture and *in vivo* animal models indicate that ET-1 and the ET_B receptor may contribute an important role in astrocyte hypertrophy, resulting in astrogliosis.

One interesting finding in the current study is that there was no ET-1–induced calcium mobilization identified in U373MG cells. This observation was further supported by our finding that inhibition of phospholipase C did not abolish ET-1–induced phosphorylation of ERK1/2. These findings indicate that classical Ca^{2+}-linked ET_A-mediated signaling is lacking in U373MG cells. It is generally considered to be the case that the ET_A receptor is coupled to $G\alpha q$, which is associated with activation of phospholipase $C\beta$ ($PLC\beta$) (64, 65). In this cell line, U373MG astrocytoma, no ET_A receptor was detectable by ligand binding assay (36) and by reverse transcription–polymerase chain reaction (66), indicating that this lack of ET_A receptor responsiveness was consistent with our finding that only the ET_B receptor antagonist BQ788 blocked ET-1–induced phosphorylation of ERK1/2 (Fig. 2). Therefore, ET-1 may not induce the activation of PKC and calcium mobilization in this cell line because of the lack of IP_3 and DAG. Moreover, the application of the PLC inhibitor U73122 did not block ET-1–induced phosphorylation of ERK1/2 (Fig. 5B). We also did not see any calcium mobilization with ET-1 treatment in this cell type (Fig. 5A), nor was the activation of the c/nPKC isoforms detected by PKC kinase assay and Western blot. Our results confirm that there is no ET_A receptor–mediated calcium mobilization induced by ET-1 in this cell type. There are some reports that ET-1 activates $G\alpha q$ coupling with ET_B receptor and mediates the variety of signaling pathways in different cells, including hepatocyte (67), vascular smooth muscle cells, C6 glioma cells, and Chinese hamster ovary cells, with stable expressing ET_B receptors (68–70), and even in astrocyte cell lines, including the

neuroblastoma cell line B103 (B103 cells) (71). In contrast to what we found in U373MG astrocytoma cells, inhibition of PLCβ completely abolished ET-1–induced ERK1/2 phosphorylation in C6 glioma cells (70), further indicating that there could be no coupling between Gαq and ET_B receptor in U373MG astrocytoma cells. The studies from other G protein-coupled receptors indicate that there are differential G protein-coupling patterns observed in different tissue and cells. For instance, the metabotropic glutamate receptors (mGluRs) are fully identified GPCRs coupling with the different G proteins. Group I receptors are coupled to Gαq to activation phospholipase C, whereas Group II and III mGluRs are coupled to $G\alpha_i$ to downregulate cAMP levels (72). $5\text{-}HT_{1A}$ receptors interacted predominantly with Gαi in the anterior raphe, whereas they were coupled to Gαo proteins in the hippocampus (73). The β3b-adrenoceptor couples to both Gαs and Gαi in CHO-K1 cells, whereas the β3a-adrenoceptor couples specifically to Gαs (74). This indicates that the differential coupling between G proteins and endothelin receptors may contribute to the variety of actions of ET-1 in different cells and tissues. Although the lack of Gαq-mediated intracellular Ca^{2+} mobilization was observed in U373MG astrocytoma cells, the rapid activation of MAPK-ERK by ET-1 was still mediated by other PTKs in a Ca^{2+}-independent manner.

PKC also plays an important role in ET-1–induced signaling, and the current study indicated that PKC was also involved in cell proliferation of U373MG cells. It has been suggested that PKC can activate upstream of the MAPK pathway at Ras or/and Raf to influence cell proliferation through the classical Ras-Raf-MAPK pathway (23, 28, 29). Although our results showed that activation of PKCs by PMA could induce phosphorylation of ERK1/2, ET-1 did not activate c/nPKCs in U373MG cells. Moreover, ET-1 did not elevate intracellular calcium through activation of PLC. The results confirmed our finding that c/nPKCs are not involved in ET-1 signaling in U373MG cells. In addition, the detection of phosphorylated ERK1/2 after pretreatment of PKC inhibitors and activation of PKCs after pretreatment with MEK1/2 inhibitors indicated that there was no "cross talk" between these two pathways. Although c/nPKCs have been ruled out in the signaling cascades induced by ET-1, the involvement of atypical PKC isoforms (ζ/τ) (29, 75, 76) might still play a role in controlling cell proliferation of U373MG cells. This needs further investigation.

In U373MG astrocytoma cells, Ras was activated following ET-1 treatment. These findings are in agreement with reports of ET-1 effects on other cell types, such as cardiac myocytes (77) and myometrial cells (23). FTI-277, an inhibitor of farnesyltransferase, increases the nonfarnesylated cytoplasmic H-Ras, which competes with active Ras and binds to Raf protein to inactivate Ras/Raf complexes (42, 43, 78, 79). Surprisingly, application of FTI-277 and introduction of the dominant negative cDNA of H-Ras into U373MG cells did not inhibit the phosphorylation of ERK1/2 induced by ET-1, whereas wild-type active H-Ras significantly stimulated the phosphorylation of ERK1/2 independent of ET-1. However, in U373MG cells, H-Ras appears not to be involved in ET-1–induced signaling. Other forms of Ras, such as K-Ras, N-Ras, or M-Ras, could play an important role in this cascade (37, 80).

In summary, the current studies indicate that ET-1–induced cell proliferation in U373MG astrocytoma cells occurs through an apparent concurrent activation of MAPK-ERK, PKC, and PI3K pathways (see Fig. 9). ET-1 activates the Ras-Raf-1-MAPK-ERK pathway without activation of PTK. In U373MG astrocytoma cells, neither c/nPKCs nor PI3K are involved in ET-1–induced ERK1/2 signaling. However, MAPK-ERK, PKC, and PI3K pathways appear to exert their roles in parallel without a direct, apparent cross talk. They do, however, appear to activate key components (e.g., common and discrete transcription factors) in the proliferation response, because inhibition of any one parallel pathway blocks proliferation. This parallel signaling is not unlikely, as the proliferation response is dependent on many cellular processes that may be activated simultaneously in tumor cell proliferation through complex signaling systems and important transcriptional events.

We wish to thank Dr. Raghu Krishnamoorthy for helpful comments on the manuscript.

1. Yorio T, Krishnamoorthy R, Prasanna G. Endothelin: is it a contributor to glaucoma pathophysiology? J Glaucoma 11:259–270, 2002.
2. Desai D, He S, Yorio T, Krishnamoorthy RR, Prasanna G. Hypoxia augments TNF-[alpha]–mediated endothelin-1 release and cell proliferation in human optic nerve head astrocytes. Biochem Biophys Res Commun 318:642–648, 2004.
3. Naidoo V, Mahabeer R, Raidoo DM. Cellular distribution of endothelin-1 mRNA in human brain by in situ RT-PCR. Metab Brain Dis 16:207–218, 2001.
4. Takahashi K, Totsune K, Kitamuro T, Sone M, Murakami O, Shibahara S. Three vasoactive peptides, endothelin-1, adrenomedullin and urotensin-II, in human tumour cell lines of different origin: expression and effects on proliferation. Clin Sci 103:35S–38S, 2002.
5. Egidy G, Eberl LP, Valdenaire O, Irmler M, Majdi R, Diserens A-C, Fontana A, Janzer R-C, Pinet F, Juillerat-Jeanneret L. The endothelin system in human glioblastoma. Lab Investig 80:1681–1689, 2000.
6. Prasanna G, Hulet C, Desai D, Krishnamoorthy RR, Narayan S, Brun A-M, Suburo AM, Yorio T. Effect of elevated intraocular pressure on endothelin-1 in a rat model of glaucoma. Pharmacol Res 51:41–50, 2005.
7. Prasanna G, Krishnamoorthy R, Clark AF, Wordinger RJ, Yorio T. Human optic nerve head astrocytes as a target for endothelin-1. Investig Ophthalmol Vis Sci 43:2704–2713, 2002.
8. Hernandez M, Nieto ML, Sanchez Crespo M. Cytosolic phospholipase A2 and the distinct transcriptional programs of astrocytoma cells. Trends Neurosci 23:259–264, 2000.
9. Hernandez MR. The optic nerve head in glaucoma: role of astrocytes in tissue remodeling. Prog Retin Eye Res 19:297–321, 2000.
10. Grant K, Loizidou M, Taylor I. Endothelin-1: a multifunctional molecule in cancer. Br J Cancer 88:163–166, 2003.
11. Schinelli S. The brain endothelin system as potential target for brain-related pathologies. Curr Drug Target CNS Neurol Disord 1:543–553, 2002.

12. Wedgwood S, Dettman RW, Black SM. ET-1 stimulates pulmonary arterial smooth muscle cell proliferation via induction of reactive oxygen species. Am J Physiol Lung Cell Mol Physiol 281:L1058–L1067, 2001.
13. Nambi P, Clozel M, Feuerstein G. Endothelin and heart failure. Heart Fail Rev 6:335–340, 2001.
14. Lazarini F, Strosberg AD, Couraud PO, Cazaubon SM. Coupling of ETB endothelin receptor to mitogen-activated protein kinase stimulation and DNA synthesis in primary cultures of rat astrocytes. J Neurochem 66:459–465, 1996.
15. Wang Y, Rose P, Webb M, Dunn M. Endothelins stimulate mitogen activated protein kinase cascade through either ETA or ETB. Am J Physiol 267:C1130–C1135, 1994.
16. Cazaubon S, Ramos-Morales F, Fischer S, Schweighoffer F, Strosberg A, Couraud P. Endothelin induces tyrosine phosphorylation and GRB2 association of Shc in astrocytes. J Biol Chem 269:24805–24809, 1994.
17. Morga E, Faber C, Heuschling P. Stimulation of endothelin B receptor modulates the inflammatory activation of rat astrocytes. J Neurochem 74:603–612, 2000.
18. Rogers S, Peters C, Pomonis J, Hagiwara H, Ghilardi J, Mantyh P. Endothelin B receptors are expressed by astrocytes and regulate astrocyte hypertrophy in the normal and injured CNS. Glia 41:180–190, 2003.
19. Peters CM, Rogers SD, Pomonis JD, Egnazyck GF, Keyser CP, Schmidt JA, Ghilardi JR, Maggio JE, Mantyh PW. Endothelin receptor expression in the normal and injured spinal cord: potential involvement in injury-induced ischemia and gliosis. Exp Neurol 180:1–13, 2003.
20. Stork PJS, Schmitt JM. Crosstalk between cAMP and MAP kinase signaling in the regulation of cell proliferation. Trends Cell Biol 12: 258–266, 2002.
21. Sugden P. An overview of endothelin signaling in the cardiac myocyte. J Mol Cell Cardiol 35:871–886, 2003.
22. Kolch W. Meaningful relationships: the regulation of the Ras/Raf/MEK/ERK pathway by protein interactions. Biochem J 351:289–305, 2000.
23. Robin P, Boulven I, Desmyter C, Harbon S, Leiber D. ET-1 stimulates ERK signaling pathway through sequential activation of PKC and Src in rat myometrial cells. Am J Physiol Cell Physiol 283:C251–C260, 2002.
24. Naicker S, Bhoola KD. Endothelins: vasoactive modulators of renal function in health and disease. Pharmacol Ther 90:61–88, 2001.
25. Shi-Wen X, Chen Y, Denton C, Eastwood M, Renzoni E, Bou-Gharios G, Pearson J, Dashwood M, DuBois R, Black C, Leask A, Abraham D. Endothelin-1 promotes myofibroblast induction through the ETA receptor via a rac/PI3 kinase/Akt-dependent pathway and is essential for the enhanced contractile phenotype of fibrotic fibroblasts. Mol Biol Cell 15:2707–2719, 2004.
26. Bisotto S, Fixman ED. Src-family tyrosine kinases, phosphoinositide 3-kinase and Gab1 regulate extracellular signal-regulated kinase 1 activation induced by the type A endothelin-1 G-protein-coupled receptor. Biochem J 360:77–85, 2001.
27. Masaki T, Miwa S, Sawamura T, Ninomiya H, Okamoto Y. Subcellular mechanisms of endothelin action in the vascular system. Eur J Pharmacol 375:133–138, 1999.
28. Clerk A, Bogoyevitch M, Anderson M, Sugden P. Differential activation of protein kinase C isoforms by endothelin-1 and phenylephrine and subsequent stimulation of p42 and p44 mitogen-activated protein kinases in ventricular myocytes cultured from neonatal rat hearts. J Biol Chem 269:32848–32857, 1994.
29. Robin P, Boulven I, Bole-Feysot C, Tanfin Z, Leiber D. Contribution of PKC-dependent and -independent processes in temporal ERK regulation by ET-1, PDGF, and EGF in rat myometrial cells. Am J Physiol Cell Physiol 286:C798–C806, 2004.
30. Coward P, Wada HG, Falk MS, Chan SDH, Meng F, Akil H, Conklin BR. Controlling signaling with a specifically designed Gi-coupled receptor. Proc Natl Acad Sci U S A 95:352–357, 1998.
31. Xu J, Weng Y-I, Simoni A, Krugh BW, Liao Z, Weisman GA, Sun GY. Role of PKC and MAPK in cytosolic PLA2 phosphorylation and arachadonic acid release in primary murine astrocytes. J Neurochem 83: 259–270, 2002.
32. Dibas A, Wood J, Mia A, Yorio T. The ATP-depleting reagent iodoacetamide induces the degradation of protein kinase C alpha (PKC alpha) in LLC-PK1 pig kidney cells. Life Sci 61:1697–1704, 1997.
33. Castro AF, Amorena C, Muller A, Ottaviano G, Tellez-Inon MT, Taquini AC. Extracellular ATP and bradykinin increase cGMP in vascular endothelial cells via activation of PKC. Am J Physiol Cell Physiol 275:C113–C119, 1998.
34. Prasanna G, Dibas AI, Yorio T. Cholinergic and adrenergic modulation of the Ca2+ response to endothelin-1 in human ciliary muscle cells. Invest Ophthalmol Vis Sci 41:1142–1148, 2000.
35. Grynkiewicz G, Poenie M, Tsien R. A new generation of Ca2+ indicators with greatly improved fluorescence properties. J Biol Chem 260:3440–3450, 1985.
36. Wu-Wong J, Chiou W, Magnuson S, Opgenorth T. Endothelin receptor in human astrocytoma U373MG cells: binding, dissociation, receptor internalization. J Pharmacol Exp Ther 274:499–507, 1995.
37. Ehrhardt A, Ehrhardt GRA, Guo X, Schrader JW. Ras and relatives—job sharing and networking keep an old family together. Exp Hematol 30:1089–1106, 2002.
38. Chong H, Vikis HG, Guan K-L. Mechanisms of regulating the Raf kinase family. Cell Signal 15:463–469, 2003.
39. Yan J, Roy S, Apolloni A, Lane A, Hancock JF. Ras isoforms vary in their ability to activate Raf-1 and phosphoinositide 3-kinase. J Biol Chem 273:24052–24056, 1998.
40. Zisoulis DG, Kansas GS. H-Ras and PI3K cooperate to induce FucT-VII expression in Jurkat T cells. J Biol Chem 279:39495–39504, 2004.
41. Schinelli S, Zanassi P, Paolillo M, Wang H, Feliciello A, Gallo V. Stimulation of endothelin B receptors in astrocytes induces cAMP response element-binding protein phosphorylation and c-fos expression via multiple mitogen-activated protein kinase signaling pathways. J Neurosci 21:8842–8853, 2001.
42. Lerner EC, Qian Y, Blaskovich MA, Fossum RD, Vogt A, Sun J, Cox AD, Der CJ, Hamilton AD, Sebti SM. Ras CAAX peptidomimetic FTI-277 selectively blocks oncogenic Ras signaling by inducing cytoplasmic accumulation of inactive Ras-Raf complexes. J Biol Chem 270: 26802–26806, 1995.
43. Upadhyay D, Correa-Meyer E, Sznajder JI, Kamp DW. FGF-10 prevents mechanical stretch-induced alveolar epithelial cell DNA damage via MAPK activation. Am J Physiol Lung Cell Mol Physiol 284:L350–L359, 2003.
44. Koyama Y, Yoshioka Y, Matsuda T, Baba A. Focal adhesion kinase is required for endothelin-induced cell cycle progression of cultured astrocytes. Glia 43:185–189, 2003.
45. Koyama Y, Yoshioka Y, Hashimoto H, Matsuda T, Baba A. Endothelins increase tyrosine phosphorylation of astrocytic focal adhesion kinase and paxillin accompanied by their association with cytoskeletal components. Neuroscience 101:219–227, 2000.
46. Hua H, Munk S, Whiteside CI. Endothelin-1 activates mesangial cell ERK1/2 via EGF-receptor transactivation and caveolin-1 interaction. Am J Physiol Renal Physiol 284:F303–F312, 2003.
47. Kawanabe Y, Masaki T, Hashimoto N. Involvement of epidermal growth factor receptor–protein tyrosine kinase transactivation in endothelin-1–induced vascular contraction. J Neurosurg 100:1066–1071, 2004.
48. Kawanabe Y, Nozaki K, Hashimoto N, Masaki T. Involvement of extracellular Ca2+ influx and epidermal growth factor receptor tyrosine kinase transactivation in endothelin-1–induced arachidonic acid release. Br J Pharmacol 139:1516–1522, 2003.
49. Imokawa G, Kobayasi T, Miyagishi M. Intracellular signaling

mechanisms leading to synergistic effects of endothelin-1 and stem cell factor on proliferation of cultured human melanocytes. Cross-talk via trans-activation of the tyrosine kinase c-kit receptor. J Biol Chem 275: 33321–33328, 2000.

50. Vacca F, Bagnato A, Catt KJ, Tecce R. Transactivation of the epidermal growth factor receptor in endothelin-1–induced mitogenic signaling in human ovarian carcinoma cells. Cancer Res 60:5310–5317, 2000.
51. Matsui T, Nagoshi T, Rosenzweig A. Akt and PI 3-kinase signaling in cardiomyocyte hypertrophy and survival. Cell Cycle 2:220–223, 2003.
52. Chang F, Lee J, Navolanic P, Steelman L, Shelton J, Blalock W, Franklin R, McCubrey J. Involvement of PI3K/Akt pathway in cell cycle progression, apoptosis, and neoplastic transformation: a target for cancer chemotherapy. Leukemia 17:590–603, 2003.
53. Lopez-Ilasaca M, Crespo P, Pellici PG, Gutkind JS, Wetzker R. Linkage of G protein-coupled receptors to the MAPK signaling pathway through PI 3-kinase gamma. Science 275:394–397, 1997.
54. Liu S, Premont RT, Kontos CD, Huang J, Rockey DC. Endothelin-1 activates endothelial cell nitric-oxide synthase via heterotrimeric G-protein βγ subunit signaling to protein kinase B/Akt. J Biol Chem 278: 49929–49935, 2003.
55. Lewerenz J, Letz J, Methner A. Activation of stimulatory heterotrimeric G proteins increases glutathione and protects neuronal cells against oxidative stress. J Neurochem 87:522–531, 2003.
56. Miyamoto Y, Yamauchi J, Itoh H. Src kinase regulates the activation of a novel FGD-1–related Cdc42 guanine nucleotide exchange factor in the signaling pathway from the endothelin A receptor to JNK. J Biol Chem 278:29890–29900, 2003.
57. Shichiri M, Sedivy JM, Marumo F, Hirata Y. Endothelin-1 is a potent survival factor for c-Myc–dependent apoptosis. Mol Endocrinol 12: 172–180, 1998.
58. Chen S, Mukherjee S, Chakraborty C, Chakrabarti S. High glucose-induced, endothelin-dependent fibronectin synthesis is mediated via NF-kappa B and AP-1. Am J Physiol Cell Physiol 284:C263–C272, 2003.
59. Iwai-Kanai E, Hasegawa K. Intracellular signaling pathways for norepinephrine- and endothelin-1–mediated regulation of myocardial cell apoptosis. Mol Cell Biochem 259:163–168, 2004.
60. Chintalgattu V, Katwa LC. Role of protein kinase Cδ in endothelin-induced Type I collagen expression in cardiac myofibroblasts isolated from the site of myocardial infarction. J Pharmacol Exp Ther 311:691–699, 2004.
61. Sugden PH, Clerk A. Endothelin signalling in the cardiac myocyte and its pathophysiological relevance. Curr Vasc Pharmacol 3:343–351, 2005.
62. Hua H, Goldberg HJ, Fantus IG, Whiteside CI. High glucose-enhanced mesangial cell extracellular signal-regulated protein kinase activation and α1(IV) collagen expression in response to endothelin-1: role of specific protein kinase C isozymes. Diabetes 50:2376–2383, 2001.
63. Rosano L, Salani D, Castro VD, Spinella F, Natali PG, Bagnato A. Endothelin-1 promotes proteolytic activity of ovarian carcinoma. Clin Sci 103:306S–309S, 2002.
64. Prasanna G, Narayan S, Krishnamoorthy RR, Yorio T. Eyeing endothelins: a cellular perspective. Mol Cell Biochem 253:71–88, 2003.
65. Adamsa JW, Brown JH. G-proteins in growth and apoptosis: lessons from the heart. Oncegene 20:1626–1634, 2001.
66. Paolillo M, Barbieri A, Zanassi P, Schinelli S. Expression of endothelins and their receptors in glioblastoma cell lines. J Neurooncol 79:1–7, 2006.
67. Jouneaux C, Mallat A, Serradeil-Le Gal C, Goldsmith P, Hanoune J, Lotersztajn S. Coupling of endothelin B receptors to the calcium pump and phospholipase C via Gs and Gq in rat liver. J Biol Chem 269:1845–1851, 1994.
68. Kawanabe Y, Hashimoto N, Masaki T. Characterization of G proteins involved in activation of nonselective cation channels by endothelin B receptor. Br J Pharmacol 136:1015–1022, 2002.
69. Kawanabe Y, Nauli SM. Involvement of extracellular Ca2+ influx through voltage-independent Ca2+ channels in endothelin-1 function. Cell Signal 17:911–916, 2005.
70. Cramer H, Schmenger K, Heinrich K, Horstmeyer A, Boning H, Breit A, Piiper A, Lundstrom K, Muller-Esterl W, Schroeder C. Coupling of endothelin receptors to the ERK/MAP kinase pathway. Roles of palmitoylation and Gαq. Eur J Biochem 268:5449–5459, 2001.
71. Kawanabe Y, Hashimoto N, Masaki T. B103 neuroblastoma cells predominantly express endothelin ETB receptor; effects of extracellular Ca2+ influx on endothelin-1–induced mitogenesis. Eur J Pharmacol 425:173–179, 2001.
72. Wroblewska B, Wegorzewska IN, Bzdega T, Olszewski RT, Neale JH. Differential negative coupling of type 3 metabotropic glutamate receptor to cyclic GMP levels in neurons and astrocytes. J Neurochem 96:1071–1077, 2006.
73. la Cour CM, El Mestikawy S, Hanoun N, Hamon M, Lanfumey L. Regional differences in the coupling of 5-hydroxytryptamine-1A receptors to G proteins in the rat brain. Mol Pharmacol 70:1013–1021, 2006.
74. Sato M, Hutchinson DS, Bengtsson T, Floren A, Langel U, Horinouchi T, Evans BA, Summers RJ. Functional domains of the mouse β3-adrenoceptor associated with differential G protein coupling. J Pharmacol Exp Ther 315:1354–1361, 2005.
75. Monick MM, Carter AB, Flaherty DM, Peterson MW, Hunninghake GW. Protein kinase C ζ plays a central role in activation of the p42/44 mitogen-activated protein kinase by endotoxin in alveolar macrophages. J Immunol 165:4632–4639, 2000.
76. Liberto GD, Dallot E, Parco IE-L, Cabrol D, Ferre F, Breuiller-Fouche M. A critical role for PKCζ in endothelin-1–induced uterine contractions at the end of pregnancy. Am J Physiol Cell Physiol 285: C599–C607, 2003.
77. Bogoyevitch M, Glennon P, Andersson M, Clerk A, Lazou A, Marshall C, Parker P, Sugden P. Endothelin-1 and fibroblast growth factors stimulate the mitogen-activated protein kinase signaling cascade in cardiac myocytes. The potential role of the cascade in the integration of two signaling pathways leading to myocyte hypertrophy. J Biol Chem 269:1110–1119, 1994.
78. Battaglia A, Pak K, Brors D, Bodmer D, Frangos JA, Ryan AF. Involvement of ras activation in toxic hair cell damage of the mammalian cochlea. Neuroscience 122:1025–1035, 2003.
79. Bolick S, Landowski T, Boulware D, Oshiro M, Ohkanda J, Hamilton A, Sebti S, Dalton W. The farnesyl transferase inhibitor, FTI-277, inhibits growth and induces apoptosis in drug-resistant myeloma tumor cells. Leukemia 17:451–457, 2003.
80. Ellis CA, Clark G. The importance of being K-Ras. Cell Signal 12:425–434, 2000.